

# Getting Information on $|U_{e3}|^2$ from Neutrino-less Double Beta Decay

Alexander Merle\* and Werner Rodejohann†

*Max-Planck-Institut für Kernphysik,  
Postfach 10 39 80, D-69029 Heidelberg, Germany*

## Abstract

We consider the possibility to gain information on the lepton mixing matrix element  $|U_{e3}|$  from an improved experimental limit on the effective neutrino mass governing neutrino-less double beta decay. We show that typically a lower limit on  $|U_{e3}|$  as a function of the smallest neutrino mass can be set. Furthermore, we give the values of the sum of neutrino masses and  $|U_{e3}|$  which are allowed and forbidden by an experimental upper limit on the effective mass. Alternative explanations for neutrino-less double beta decay, Dirac neutrinos or unexplained cosmological features would be required if future measurements showed that the values lie in the respective regions. Moreover, we show that a measurement of  $|U_{e3}|$  from neutrino-less double beta decay is very difficult due to the expected errors on the effective mass and the oscillation parameters.

---

\*email: alexander.merle@mpi-hd.mpg.de

†email: werner.rodejohann@mpi-hd.mpg.de

# 1 Introduction

In the next decade, neutrino physics [1] is bound to answer several crucial questions. Most interesting are in particular the ones about the magnitude of the last unknown mixing parameter  $U_{e3}$  and the one about the possible Majorana nature of the neutrino. The magnitude of  $|U_{e3}|$  is crucial for the future experimental program of neutrino physics, since in neutrino oscillation experiments the search for  $CP$  violation and partly the determination of the neutrino mass hierarchy depends on it [2]. Its value is also an important criterion in order to rule out the many models for neutrino masses and mixing [3]. Information on  $|U_{e3}|$  can be obtained by

- direct searches in reactor neutrino experiments [4];
- studies with future long-baseline neutrino experiments [5], even including  $\beta$ -beams or neutrino factories [6];
- observation of supernova neutrinos [7];
- observation of fluxes (or flux ratios) of high-energy neutrinos in neutrino telescopes [8].

In what regards the Majorana nature of the neutrino, only experiments looking for neutrino-less double beta decay ( $0\nu\beta\beta$ ) [9] are realistic possibilities, as other lepton number violating processes are far beyond reach [10]. The life-time of (or a lower limit on)  $0\nu\beta\beta$  is translated into a value (or an upper limit) of the effective mass

$$|m_{ee}| = \left| \sum U_{ei}^2 m_i \right|. \quad (1)$$

Here  $m_i$  with  $i = 1, 2, 3$  are the neutrino masses and  $U$  is the Pontecorvo-Maki-Nagakawa-Sakata (PMNS) lepton mixing matrix. From the Heidelberg-Moscow experiment the current limit on the half-life of  $^{76}\text{Ge}$  is  $1.9 \cdot 10^{25}$  y at 90 % C.L. [11], translating into a limit on the effective mass of  $|m_{ee}| \leq 0.35 \zeta$  eV, where  $\zeta$  is of  $\mathcal{O}(1)$  and denotes the nuclear matrix element uncertainty. Being the best limit for many years, the values are beginning to be challenged by the CUORICINO experiment working with  $^{130}\text{Te}$  ( $T_{1/2} \geq 3 \cdot 10^{24}$  y) [12] and the NEMO 3 experiment working with  $^{100}\text{Mo}$  ( $T_{1/2} \geq 5.8 \cdot 10^{23}$  y) and  $^{82}\text{Se}$  ( $T_{1/2} \geq 1.2 \cdot 10^{23}$  y) [13]. Other approaches such as EXO-200 [14] or GERDA [15] will soon do the same. Apart from proving the Majorana nature of neutrinos, the value of  $|m_{ee}|$  depends on 7 of the 9 parameters of low energy neutrino physics, which implies that a large amount of information is encoded in a measurement of or a limit on the effective mass. Furthermore, in the charged lepton basis,  $|m_{ee}|$  is the  $ee$  element of the neutrino mass matrix. These interesting features render the effective mass – in connection with future precision measurements of the other parameters – also a very helpful criterion to rule out models [16].

Many authors have studied the predictions for  $|m_{ee}|$  [16, 17, 18, 19, 20, 21] and how a measurement or an improved limit of neutrino-less double beta decay will allow to probe the

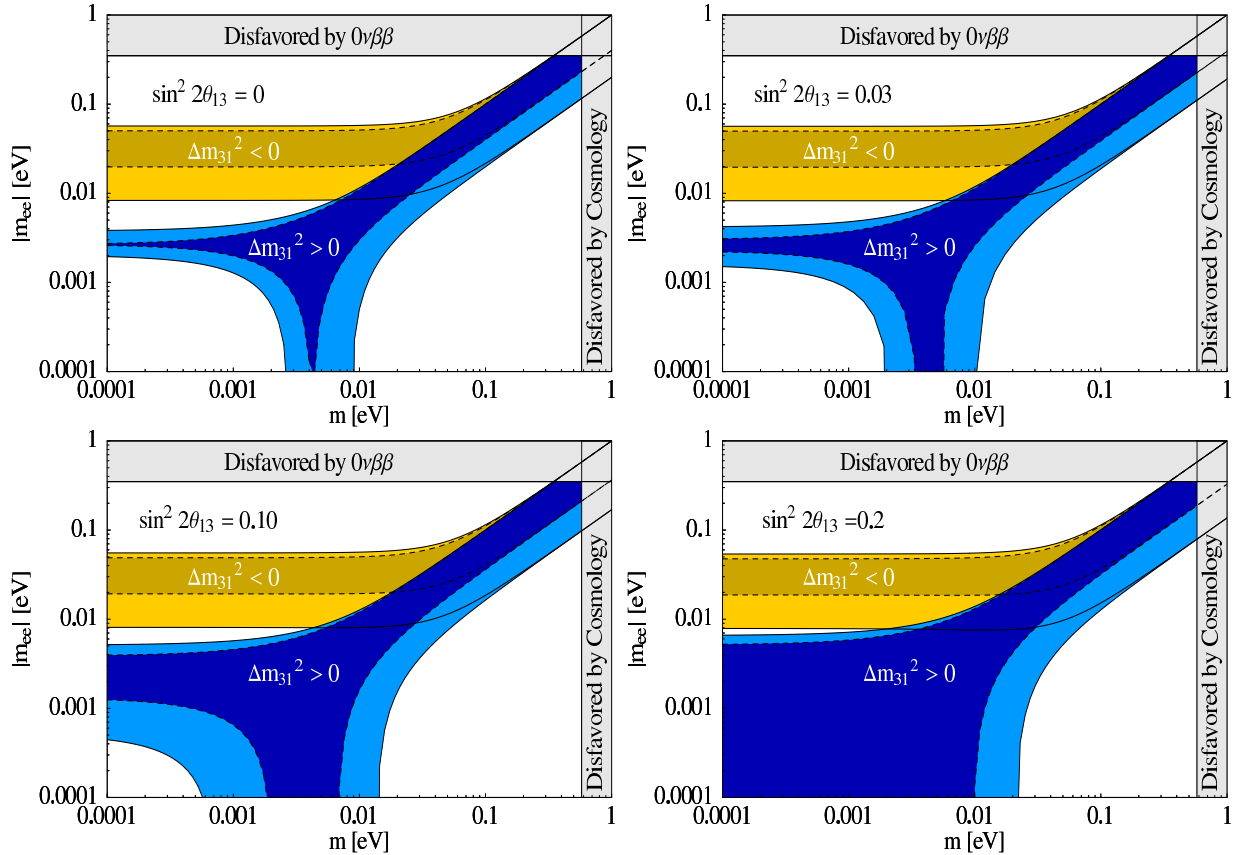


Figure 1: The effective mass as a function of the smallest neutrino mass for the normal and inverted ordering and for different values of  $|U_{e3}|^2$ . The dark regions are for the best-fit values of the other oscillation parameters, the light regions for their  $3\sigma$  values.

parameters of neutrino physics, in particular the scale and ordering of neutrino masses and the  $CP$  parameters<sup>1</sup>. A recent review can be found in Ref. [23]. Here we will concentrate on the possibility [18] to obtain information on the parameter  $|U_{e3}|^2$  from an improved limit on the effective mass. In case of a vanishing effective mass, this has been first discussed in Ref. [21].

To motivate this analysis, we show in Fig. 1 the usual plot of the effective mass as a function of the smallest neutrino mass. Both possible signs of the atmospheric mass-squared difference are taken, and the best-fit values of  $\theta_{12}$ ,  $\Delta m_{\odot}^2$ , and  $\Delta m_{\text{A}}^2$  as well as their currently allowed  $3\sigma$  ranges are used. We have chosen four different values of  $|U_{e3}|^2$ , and the difference between these cases is obvious [20]. Therefore the possibility to obtain information on  $|U_{e3}|^2$  via neutrino-less double beta decay is definitely present. As we will elaborate on in the course of this letter, a lower limit on  $|U_{e3}|^2$  as a function of the smallest neutrino mass can be set from an upper limit on the effective mass  $|m_{ee}|$ . We partly update the results

<sup>1</sup>The predictions for the remaining five elements of the neutrino mass matrix were studied in Ref. [22].

from Ref. [18]. Moreover, regions in the parameter space of  $|U_{e3}|^2$  and the sum of neutrino masses (as measurable in cosmology), which contain their allowed and forbidden values, are identified. This could be used, for instance, to perform a consistency check of future measurements of neutrino masses,  $|U_{e3}|^2$ , and  $|m_{ee}|$  in order to rule out or constrain alternative mechanisms of neutrino-less double beta decay, to show that neutrinos are Dirac particles, or to find inconsistencies in cosmological methods and models. In Ref. [20] it was shown how the value of  $|U_{e3}|^2$  influences the possibility to distinguish the normal from the inverted mass ordering with a measurement of or limit on neutrino-less double beta decay. Here we turn round the argumentation and investigate the information on  $|U_{e3}|^2$  which can be obtained by neutrino-less double beta decay. All in all, the dependence of  $|m_{ee}|$  on  $|U_{e3}|^2$  is weaker than on the other relevant parameters. It is however a worthy exercise to investigate inasmuch the two most interesting parameters of neutrino physics,  $|U_{e3}|^2$  and the effective mass, are phenomenologically connected. We finally quantify for the first time that a measurement of  $|U_{e3}|^2$  via  $0\nu\beta\beta$  is extremely challenging due to the expected experimental errors. We should remark here that the implications we are discussing rely – of course – on neutrinos being Majorana particles.

To set the stage of our discussion, we parameterize the PMNS matrix as

$$U = \begin{pmatrix} c_{12} c_{13} & s_{12} c_{13} & s_{13} e^{-i\delta} \\ -s_{12} c_{23} - c_{12} s_{23} s_{13} e^{i\delta} & c_{12} c_{23} - s_{12} s_{23} s_{13} e^{i\delta} & s_{23} c_{13} \\ s_{12} s_{23} - c_{12} c_{23} s_{13} e^{i\delta} & -c_{12} s_{23} - s_{12} c_{23} s_{13} e^{i\delta} & c_{23} c_{13} \end{pmatrix} \text{diag}(1, e^{i\alpha}, e^{i(\beta+\delta)}) , \quad (2)$$

where  $s_{ij} = \sin \theta_{ij}$ ,  $c_{ij} = \cos \theta_{ij}$ . We have one Dirac phase  $\delta$  and two Majorana phases [24]  $\alpha$  and  $\beta$ . The following best-fit values and  $3\sigma$  ranges of the oscillation parameters have been obtained [25]:

$$\begin{aligned} \Delta m_{\odot}^2 &= m_2^2 - m_1^2 = (7.9_{-0.8}^{+1.0}) \cdot 10^{-5} \text{ eV}^2 , \\ \sin^2 \theta_{12} &= 0.30_{-0.06}^{+0.10} , \\ \Delta m_{\text{A}}^2 &= |m_3^2 - m_1^2| = (2.5_{-0.6}^{+0.7}) \cdot 10^{-3} \text{ eV}^2 , \\ \sin^2 \theta_{23} &= 0.50_{-0.16}^{+0.18} , \\ |U_{e3}|^2 &= 0_{-0.000}^{+0.041} . \end{aligned} \quad (3)$$

Crucial for the form of the neutrino mass matrix and the value of the effective mass is the mass ordering, which can be normal or inverted:

$$\begin{aligned} \text{normal: } m_3 > m_2 > m_1 & \text{ with } m_2 = \sqrt{m_1^2 + \Delta m_{\odot}^2} ; \quad m_3 = \sqrt{m_1^2 + \Delta m_{\text{A}}^2} , \\ \text{inverted: } m_2 > m_1 > m_3 & \text{ with } m_2 = \sqrt{m_3^2 + \Delta m_{\odot}^2 + \Delta m_{\text{A}}^2} ; \quad m_1 = \sqrt{m_3^2 + \Delta m_{\text{A}}^2} . \end{aligned} \quad (4)$$

Of special interest are the following three extreme cases:

$$\text{normal hierarchy (NH):} \quad m_3 \simeq \sqrt{\Delta m_{\text{A}}^2} \gg m_2 \simeq \sqrt{\Delta m_{\odot}^2} \gg m_1 , \quad (5)$$

$$\text{inverted hierarchy (IH):} \quad m_2 \simeq m_1 \simeq \sqrt{\Delta m_A^2} \gg m_3 , \quad (6)$$

$$\text{quasi-degeneracy (QD):} \quad m_0^2 \equiv m_1^2 \simeq m_2^2 \simeq m_3^2 \gg \Delta m_A^2 . \quad (7)$$

Having defined the framework, we turn now to the possibility to gain information on  $|U_{e3}|^2$  from neutrino-less double beta decay.

## 2 Constraints on $|U_{e3}|^2$ from Neutrino-less Double Beta Decay

Within our parametrization from Eq. (2), the effective mass as measurable in neutrino-less double beta decay is given by

$$|m_{ee}| = \left| m_1 c_{12}^2 c_{13}^2 + m_2 s_{12}^2 c_{13}^2 e^{2i\alpha} + m_3 s_{13}^2 e^{2i\beta} \right| . \quad (8)$$

With writing Eq. (8) as

$$\begin{aligned} |m_{ee}| &= c_{13}^2 |f(m_1, m_2, \theta_{12}, \alpha, \beta) + m_3 \tan^2 \theta_{13}| \\ \text{with } f(m_1, m_2, \theta_{12}, \alpha, \beta) &= (m_1 c_{12}^2 + m_2 s_{12}^2 e^{2i\alpha}) e^{-2i\beta} , \end{aligned} \quad (9)$$

it is obvious that from an experimental upper limit on  $|m_{ee}|$  a lower limit on  $|U_{e3}|^2$  can be obtained if [18]

$$|f(m_1, m_2, \theta_{12}, \alpha, \beta)| \geq m_3 \tan^2 \theta_{13} . \quad (10)$$

Note that the absolute value of the function  $f$ , and therefore the lower limit on  $|U_{e3}|^2$ , does not depend on the Majorana phase  $\beta$ . We now show that for the inverted mass ordering and for quasi-degenerate neutrinos the condition (10) is always fulfilled: using that  $\Delta m_\odot^2 = m_2^2 - m_1^2$  and  $\Delta m_A^2 = |m_3^2 - m_1^2|$ , it is easy to see that

$$|f| \geq m_1 - s_{12}^2 (m_2 + m_1) \simeq \begin{cases} \sqrt{\Delta m_A^2} \left( \cos 2\theta_{12} (1 - \frac{1}{2} \eta) + \frac{1}{2} s_{12}^2 R \right) & \text{for IH ,} \\ m_0 (c_{12}^2 - s_{12}^2 (1 + r_\odot)) & \text{for QD .} \end{cases} \quad (11)$$

We have defined here the small parameters  $R \equiv \Delta m_\odot^2 / \Delta m_A^2$ ,  $\eta \equiv m_3^2 / \Delta m_A^2$  (in case of IH), and  $r_\odot = \frac{1}{2} \Delta m_\odot^2 / m_0^2$  (in case of QD). The left-hand side of Eq. (10) reads for IH  $\sqrt{\Delta m_A^2} \sqrt{\eta} \tan^2 \theta_{13}$  and for QD  $m_0 (1 \pm r_A) \tan^2 \theta_{13}$ , where  $r_A \equiv \frac{1}{2} \Delta m_A^2 / m_0^2$ , the plus (minus) sign is for a normal (inverted) ordering, and we have chosen  $m_1 = m_0$ . These values are much smaller than the corresponding values in Eq. (11). Therefore the condition in Eq. (10) is always fulfilled for IH and QD, and a lower limit on  $|U_{e3}|^2$  can always be obtained in these cases.

The situation is different in case of a normal hierarchy. For instance, if we neglect  $m_1$ , then Eq. (10) translates into  $\sqrt{\Delta m_A^2} \tan^2 \theta_{13} \leq \sqrt{\Delta m_\odot^2} \sin^2 \theta_{12}$ . The  $3\sigma$ -limit on  $\tan^2 \theta_{13}$

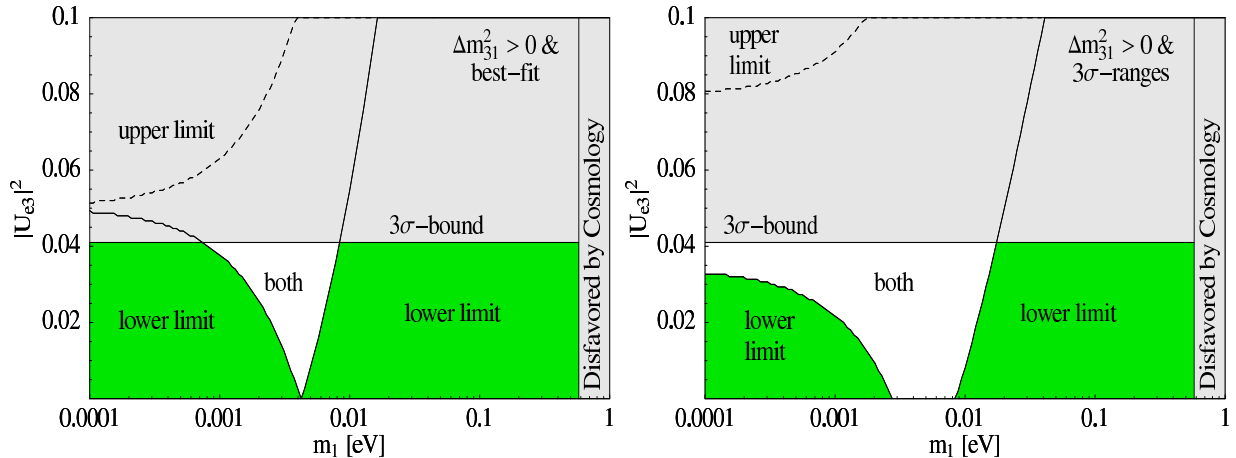


Figure 2: Regions in the  $m_1$ - $|U_{e3}|^2$ -plane in which upper and lower limits on  $|U_{e3}|^2$  can be obtained. In the white region both is possible, depending in particular on the Majorana phases. The left plot is for the best-fit values of the oscillation parameters, the right plot for the current  $3\sigma$  ranges, in both we have also indicated the current  $3\sigma$  bound on  $|U_{e3}|^2$ .

is 0.043. For the best-fit values of  $\theta_{12}$  and the mass-squared differences the condition (10) is fulfilled. Consequently, a lower limit on  $|U_{e3}|^2$  could be set. However, for the values  $\Delta m_{\odot}^2 = 7.4 \cdot 10^{-5} \text{ eV}^2$ ,  $\Delta m_{\text{A}}^2 = 2.9 \cdot 10^{-3} \text{ eV}^2$ , and  $\sin^2 \theta_{12} = 0.25$ , the condition (10) is not fulfilled, i.e., an upper limit on  $|U_{e3}|^2$  can be obtained [18]. The lesson is that there are situations in which small offsets of the values of the oscillation parameters lead to different scenarios in what regards a limit on  $|U_{e3}|^2$ . This is of course also true if  $m_1$  is small but non-zero, in which case the values of both Majorana phases also play a crucial role. In Fig. 2 we show in green (or, in a black and white printout, dark grey) the regions in the  $m_1$ - $|U_{e3}|^2$ -plane in which a lower limit on  $|U_{e3}|^2$  can be obtained. In the white region both, a lower and an upper limit are possible, depending on the precise values of  $m_{1,2,3}$ ,  $\alpha$ ,  $\beta$ , and  $\theta_{12}$ . If  $m_1$  approaches values in which neutrinos become quasi-degenerate, then – as discussed above – a lower limit is always obtainable. The left plot is for the best-fit values of  $\sin^2 \theta_{12}$  and the mass-squared differences, the right plot for their currently allowed  $3\sigma$ -ranges. Note that there are also regions in which regardless of the values of  $m_1$ ,  $\alpha$ , and  $\theta_{12}$  an upper limit can be obtained. They are located in the upper left corner of the plots, above the dashed line. We have calculated this upper limit for various possible bounds on  $|m_{ee}|$ . As it turns out, even for an extremely small bound of  $1 \cdot 10^{-4} \text{ eV}$  the upper limit lies well above the current experimental limit on  $|U_{e3}|^2$ . Therefore, this possibility will not be considered.

For the remainder of the paper we will always assume that the condition Eq. (10) is fulfilled so that a lower limit on  $|U_{e3}|^2$  can result. One should keep in mind that for part of the  $m_1$ - $|U_{e3}|^2$ -plane in case of a normal hierarchy (i.e., small  $m_1$ ), this condition might not be fulfilled. However, such small values of  $m_1$  will be measured not before the very far future [9].

As clear from the above discussion, and in particular from Eq. (10), an experimental bound on the effective mass leads to

$$|m_{ee}| \geq c_{13}^2 |f| - m_3 s_{13}^2 . \quad (12)$$

This translates into a lower bound on  $|U_{e3}|^2$ , reading

$$|U_{e3}|^2 \geq \frac{|f| - |m_{ee}|}{|f| + m_3} , \quad (13)$$

where  $|f|$  is explicitly given by

$$|f|^2 = m_1^2 c_{12}^4 + m_2^2 s_{12}^4 + 2 \cos 2\alpha m_1 m_2 s_{12}^2 c_{12}^2 . \quad (14)$$

The lowest allowed  $|U_{e3}|^2$  is independent on the Majorana phase  $\beta$ , but a function of the Majorana phase  $\alpha$ . We are interested here in the parameter space of neutrino mass and  $|U_{e3}|^2$ . It turns out that the covered area in this parameter space is maximized for  $\alpha = 0$ , and minimized for  $\alpha = \pi/2$ . As the Majorana phase is unknown, one has to take the weakest condition, i.e.,  $\alpha = \pi/2$ . This is a special value, as in case of an inverted hierarchy it is associated with the conservation of the flavor symmetry  $L_e - L_\mu - L_\tau$  [26] and for IH and QD it guarantees stability of  $\theta_{12}$  with respect to radiative corrections [27]. Moreover, large cancellations in the effective mass are resulting:

$$|m_{ee}|_{\alpha=\pi/2} \simeq \begin{cases} \sqrt{\Delta m_A^2} c_{13}^2 \cos 2\theta_{12} & \text{IH} , \\ m_0 (\cos 2\theta_{12} + |U_{e3}|^2 (\cos 2\beta - \cos 2\theta_{12})) & \text{QD} , \end{cases}$$

to be compared with the maximal possible values  $\sqrt{\Delta m_A^2} c_{13}^2$  and  $m_0$ , respectively. It is instructive to evaluate the bound (13) in case of the three extreme mass hierarchies NH, IH and QD:

**NH:** using  $m_3^2 \simeq \Delta m_A^2 (1 + \eta)$  and  $m_2^2 \simeq \Delta m_A^2 (R + \eta)$ , where  $\eta = m_1^2/\Delta m_A^2$  and  $R = \Delta m_\odot^2/\Delta m_A^2$ , it follows

$$|U_{e3}|^2 \gtrsim \frac{w - |m_{ee}|/\sqrt{\Delta m_A^2}}{1 + \frac{1}{2}\eta + w} , \quad \text{where } w = \sqrt{\eta c_{12}^4 + (R + \eta) s_{12}^4 + 2 c_{2\alpha} \sqrt{\eta R} s_{12}^2 c_{12}^2} . \quad (15)$$

In the extreme case we can neglect  $\eta$  and get

$$|U_{e3}|^2 \gtrsim \sqrt{R} s_{12}^2 - \frac{|m_{ee}|}{\sqrt{\Delta m_A^2}} . \quad (16)$$

Recall that for certain values of  $\sqrt{R}$  and  $s_{12}^2$  a lower limit is not possible.

**IH:** for the inverted mass hierarchy it holds  $m_1^2 = m_3^2 + \Delta m_A^2$  and  $m_2^2 = m_1^2 + \Delta m_\odot^2 = \Delta m_A^2 + \Delta m_\odot^2 + m_3^2$ . Neglecting  $m_3$  and  $\Delta m_\odot^2$  it follows

$$|U_{e3}|^2 \gtrsim 1 - \frac{|m_{ee}|}{\sqrt{\Delta m_A^2} \sqrt{1 - \sin^2 2\theta_{12} \sin^2 \alpha}}. \quad (17)$$

**QD:** in the region of quasi-degenerate neutrinos, using  $m_0 \equiv m_1 \simeq m_2 \simeq m_3$ , we have

$$|U_{e3}|^2 \gtrsim \frac{\sqrt{1 - \sin^2 2\theta_{12} \sin^2 \alpha} - |m_{ee}|/m_0}{1 + \sqrt{1 - \sin^2 2\theta_{12} \sin^2 \alpha}}. \quad (18)$$

In the last two cases it is obvious that the limit is strongest for  $\alpha = 0$ , in the sense that more parameter space could be excluded for this value of  $\alpha$ . In Fig. 3 we show the results of a detailed numerical analysis – using the exact formulae – of the possibility to obtain information on  $|U_{e3}|^2$  with neutrino-less double beta decay in case of a normal mass ordering. Different experimental limits  $m_{\text{exp}}$  on the effective mass are assumed. The white area in Fig. 3 is the one in which an upper or lower limit on  $|U_{e3}|^2$  could be set, depending on the precise values of the oscillation parameters, neutrino masses, and Majorana phases. This area corresponds to the white  $3\sigma$ -region in Fig. 2. It is separated by the dashed line from the green area (medium grey), which is marked with “allowed” and contains the allowed values of  $m_1$  and  $|U_{e3}|^2$ . The green (medium grey) and white areas are the same as in the right plot of Fig. 2. The point is that for a limit on  $|m_{ee}|$ , denoted here  $m_{\text{exp}}$ , these areas become smaller because the yellow and red areas cut into them: The dark yellow (darkest grey) area marked by “BF” between the solid lines is the range of the lower limit on  $|U_{e3}|^2$  if  $\Delta m_\odot^2$ ,  $\Delta m_A^2$ , and  $\theta_{12}$  are fixed to their best-fit values. If these parameters are allowed to vary within their  $3\sigma$ -ranges, then this area grows, and it is given by the light yellow (lightest grey) area between the dotted lines, marked with “ $3\sigma$ ”. As mentioned above, the limit on  $|U_{e3}|^2$  is a function of the Majorana phase  $\alpha$  (cf. Eq. (13)). The lower limit is therefore not a sharp line, but an area because of its variation with  $\alpha$ . We indicated in the plot the extreme cases  $\alpha = \pi/2$  and  $\alpha = 0$ . As mentioned above, for the latter value more parameter space can be covered, as the respective curve (solid for the best-fit parameters, dotted for the  $3\sigma$ -ranges) is to the left of the line for  $\alpha = \pi/2$ . The red (darkest) region is the one which is incompatible with the measured limit of  $|m_{ee}|$ . If the limit on  $|m_{ee}|$  decreases, the excluded area increases of course. If the limit becomes very small, i.e., below 0.001 eV, then large part of the  $m_1$ - $|U_{e3}|^2$ -plane can be excluded. In plots like the ones in Fig. 1 such small values of  $|m_{ee}|$  correspond to the “chimney”, in which the value of the effective mass sharply drops and only a certain range for  $m_1$  is allowed.

Now we turn to the inverted mass ordering. Here the parameter space is defined by  $m_3$  and  $|U_{e3}|^2$ . Fig. 4 displays the result of our detailed analysis. The green (medium grey) area, marked with “allowed”, in Fig. 4 is allowed by the respective limit  $m_{\text{exp}}$  on the effective mass. There is – in contrast to the case of a normal hierarchy in Fig. 3 – no white area,



because for the inverted ordering there is always a lower limit possible. The dark yellow (darkest grey) area marked by “BF” between the solid lines is the range of the lower limit on  $|U_{e3}|^2$  if  $\Delta m_{\odot}^2$ ,  $\Delta m_{\text{A}}^2$ , and  $\theta_{12}$  are fixed to their best-fit values. If these parameters are allowed to vary within their  $3\sigma$ -ranges, then this area grows, and it is given by the light yellow (lightest grey) area between the dotted lines, marked with “ $3\sigma$ ”. As the limit on  $|U_{e3}|^2$  is a function of the Majorana phase  $\alpha$ , the lower limit is not a sharp line, but an area. We indicated in the plot the extreme cases  $\alpha = \pi/2$  and  $\alpha = 0$ , and again for the latter value more parameter space can be covered. Parameters lying in the red (darkest) region are incompatible with the measured limit of  $|m_{ee}|$ . In general, the excluded area is larger than for the normal ordering shown in Fig. 3, as long as the limit on  $|m_{ee}|$  is the same, e.g. for  $m_{\text{exp}} = 0.01$  eV. However, for values of  $|m_{ee}|$  smaller than around 0.008 eV (cf. Fig. 1), the inverted mass ordering is excluded anyway, and no information can be got for that case. For a limit on  $|m_{ee}|$  of 0.1 eV we are in the quasi-degenerate regime, and the corresponding plot looks identical to the one in the normal mass ordering in Fig. 3.

For a limit on  $|m_{ee}|$  of 0.01 eV there is no best-fit area anymore. The reason is that (neglecting  $m_3 |U_{e3}|^2$ ) the effective mass is larger than  $c_{13}^2 \sqrt{\Delta m_{\text{A}}^2} \cos 2\theta_{12}$ , which for the best-fit values of  $\Delta m_{\text{A}}^2$  and  $\theta_{12}$  is  $0.02 c_{13}^2$  eV. With  $c_{13}^2 \gtrsim 0.96$  one cannot reach 0.01 eV. If the experimental limit becomes smaller than roughly 0.06 eV, one enters the horizontal band in Fig. 1, in which the effective mass is basically independent of  $m_3$ . Decreasing the bound down to the minimal  $|m_{ee}|$  of 0.048 eV will therefore strongly constrain  $|U_{e3}|^2$ . These considerations are indeed confirmed by the plots.

In Fig. 5 we concentrate on the forbidden (red or dark grey) and allowed (green or medium grey) regions of  $|U_{e3}|^2$  and of the sum  $\Sigma = \sum m_i$  of neutrino masses. Cosmological observations are sensitive to this observable, and current limits of order 1 eV are expected to be improved considerably [28]. Our quite conservative example bound is  $\Sigma < 1.74$  eV from Ref. [29]. The current  $3\sigma$  limit on  $|U_{e3}|^2$  is also indicated in the plots. We consider different limits  $m_{\text{exp}}$  on the effective mass and show both cases, normal and inverted mass ordering. There is a lower limit on  $\Sigma = \sum m_i$  given by  $\sqrt{\Delta m_{\text{A}}^2} + \sqrt{\Delta m_{\odot}^2}$  (normal ordering) and  $2\sqrt{\Delta m_{\text{A}}^2}$  (inverted ordering), also shown in the plot. The regions have been obtained using  $\alpha = \frac{\pi}{2}$  and the best-fit value of  $\sin^2 \theta_{12} = 0.30$ . The choice  $\alpha = \frac{\pi}{2}$  is the most conservative case in the sense that, for other values of  $\alpha$ , an even larger area could be excluded. In turn, the red (dark grey) region is forbidden independently of the exact value of the Majorana phase  $\alpha$ . We have also indicated how the areas change when  $\sin^2 \theta_{12}$  is not the current best-fit value. For its upper and lower  $3\sigma$  limits the allowed (red or dark grey) and forbidden (green or medium grey) areas would be separated by the dashed line ( $\sin^2 \theta_{12} = 0.24$ ) and the dotted line ( $\sin^2 \theta_{12} = 0.40$ ).

Knowledge of the solar mixing angle is obviously needed to give stronger constraints. Note that the upper two plots in Fig. 5 have been drawn for an experimental limit on the effective mass of  $m_{\text{exp}} = 0.01$  eV, which is expected to be achieved, e.g., by GERDA within 3 years of running [15]. Hence, after that period one could, with a better knowledge on  $s_{12}^2$ , exclude about half of the  $|U_{e3}|^2$ - $\Sigma$ -parameter space (or even more) from a *non*-observation

of neutrino-less double beta decay. There is a strong dependence on  $s_{12}^2$  for this value of  $m_{\text{exp}}$ . For a better limit from double beta experiments, the exact value of the solar neutrino mixing angle would be less important to give constraints. The precision of  $\theta_{12}$  is however quite important for limits on  $|m_{ee}|$  in the regime of 0.1 eV.

The information obtained on  $|U_{e3}|^2$  summarized in Figs. 3, 4, and 5 assumes that only light neutrino exchange is responsible for neutrino-less double beta decay. From those, Figure 5 is better suited for consistency checks and looking for alternative mechanism of  $0\nu\beta\beta$ . For instance, suppose that future data shows that  $\sin^2\theta_{12} = 0.30$  to a good precision (this is quite plausible as it is the best known mixing parameter). In addition, let us assume that a limit of 0.1 eV on the effective mass is established and that  $\Sigma = 0.8$  eV is inferred from cosmology. If  $|U_{e3}|^2 = 0.04$  is measured, then everything is consistent. In contrast, if a reactor neutrino experiment shows that  $|U_{e3}|^2 = 0.01$ , then we are in the excluded region. In this case – assuming that neutrino oscillation physics is described by standard 3-flavor physics – the following possibilities are present: (i) neutrinos are Dirac particles; (ii) cosmology has unexplained features mimicking effects of neutrino masses; (iii) there is a mechanism besides light neutrino exchange which contributes significantly to  $0\nu\beta\beta$  and whose amplitude interferes destructively with it. The first item could be checked by a KATRIN measurement corresponding to a neutrino mass of  $\simeq \Sigma/3 \simeq 0.27$ , which is above the claimed sensitivity of 0.2 eV [30]. The last item might be indirectly checked if R-parity violating SUSY is contributing to  $0\nu\beta\beta$  [31]. In this case, the relevant parameters such as sparticle masses and their coupling constants with particles may be inferred from collider experiments. Many more examples in this spirit can be read off from Fig. 5.

It is now the right time to mention the uncertainty stemming from the Nuclear Matrix Elements (NMEs), which will be the dominating error in what regards the extraction of physics parameters from  $|m_{ee}|$ . We can write the decay width of neutrino-less double beta decay as  $\Gamma = x |m_{ee}|^2$ , where  $x = G(E_0, Z) |\mathcal{M}|^2$  contains the phase space factor  $G(E_0, Z)$  – which is a calculable function of the nucleus – and the nuclear matrix element  $|\mathcal{M}|^2$ . If  $\sqrt{x}$  goes from  $y$  to  $\zeta y$ , where  $\zeta$  is the NME uncertainty, then the uncertainty on  $|m_{ee}|$  is [16, 19]

$$\Delta(|m_{ee}|) \equiv \frac{|m_{ee}|^{\text{max}} - |m_{ee}|^{\text{min}}}{|m_{ee}|^{\text{max}} + |m_{ee}|^{\text{min}}} = \frac{\zeta - 1}{\zeta + 1}. \quad (19)$$

Of course, in what regards the limit on  $|U_{e3}|^2$ , the NME uncertainty can simply be taken into account by modifying the experimental limit on  $|m_{ee}|$  accordingly, which enables us to read off the influence of such uncertainties directly from Figs. 3 and 4. Recall that the bounds on  $|U_{e3}|^2$  are very sensitive to the limit of  $|m_{ee}|$  in case of an inverted hierarchy. For instance, in Fig. 4 the change between the limits  $|m_{ee}| \leq 0.06$  eV and  $|m_{ee}| \leq 0.05$  eV is – as discussed above – quite dramatic. On the other hand, between the values  $|m_{ee}| \leq 0.1$  eV and  $|m_{ee}| \leq 0.06$  eV there is not much difference. Nevertheless, this indicates that the possible impact of the NME uncertainty in what regards information on  $|U_{e3}|^2$  depends crucially on the value of the effective mass. We can estimate that in case the inverted mass

hierarchy regime is touched by experiments ( $|m_{ee}|$  smaller than 0.05 eV), NME uncertainties smaller than 20% are necessary for robust limits and exclusion areas. For smaller limits on  $|m_{ee}|$ , uncertainties up to a factor 2 are still allowed, as they render the excluded areas rather robust.

Much more crucial will the uncertainty be if one wants to *measure*  $|U_{e3}|^2$ . As an example, consider the inverted hierarchy in the limit of vanishing  $m_3 |U_{e3}|^2$ . As can be seen from Fig. 1, this approximation is valid for  $m_3 \lesssim 0.01$  eV. In this case the formula

$$|U_{e3}|^2 = 1 - \frac{|m_{ee}|}{\sqrt{\Delta m_A^2} \sqrt{1 - \sin^2 2\theta_{12} \sin^2 \alpha}} \quad (20)$$

can easily be obtained. Simple error propagation yields

$$\begin{aligned} \sigma(|U_{e3}|^2) = & \frac{|m_{ee}|}{2\sqrt{\Delta m_A^2} (1 - \sin^2 2\theta_{12} s_\alpha^2)^{3/2}} \left[ (1 - \sin^2 2\theta_{12} s_\alpha^2)^2 \left( \frac{\sigma(\Delta m_A^2)}{\Delta m_A^2} \right)^2 + \right. \\ & \left. + 4 \left( 4 \cos^2 2\theta_{12} s_{12}^4 s_\alpha^4 \left( \frac{\sigma(s_{12}^2)}{s_{12}^2} \right)^2 + (1 - \sin^2 2\theta_{12} s_\alpha^2)^2 \left( \frac{\sigma(|m_{ee}|)}{|m_{ee}|} \right)^2 \right) \right]^{1/2}. \end{aligned} \quad (21)$$

In Fig. 6 we plot  $\sigma(|U_{e3}|^2)$  and  $\sigma(|U_{e3}|^2)/|U_{e3}|^2$  while taking relative errors of 5 and 10 % for  $\Delta m_A^2$  and  $\sin^2 \theta_{12}$ , respectively [2]. In what regards the effective mass, we assume an experimental error  $\sigma(|m_{ee}|)/|m_{ee}|$  of 20 %. The error shows a strong dependence on the Majorana phase  $\alpha$ . Interestingly, especially the value of  $\alpha = \frac{\pi}{2}$ , which allowed to set the realistic lower limit on  $|U_{e3}|^2$  for a non-observation of neutrino-less double beta decay, is the most conservative case for a  $|U_{e3}|^2$ -measurement. The relative error would be nearly 25 % in that case, but can also go down to approximately 5 % for  $\alpha = 0$ , which would then be comparable to the current knowledge of the oscillation parameters. However, as the absolute error on  $|U_{e3}|^2$  is larger than the currently allowed  $3\sigma$ -bound, we conclude that a measurement of this parameter via  $0\nu\beta\beta$  is very difficult, simply due to lack of knowledge on the Majorana phase  $\alpha$ .

The NME uncertainty  $\zeta$  can be taken into account by using [19]  $|m_{ee}| = \zeta |m_{ee}|_{\min}^{\text{exp}}$ , where  $|m_{ee}|_{\min}^{\text{exp}}$  is obtained from the measurement of  $0\nu\beta\beta$  when the largest NME is used. Then, one simply gets a factor of  $\zeta$  in front of Eq. (21), which can maybe double the error, but does not change the order of magnitude. This is illustrated in Fig. 7, where we show  $\sigma(|U_{e3}|^2)$  as a function of  $\alpha$  and  $\zeta$  for two examples of the errors on the oscillation parameters. However, for advantageous values of  $\alpha$ , one can get a reasonable measurement of  $\sigma(|U_{e3}|^2)$ , but therefore, external information on the Majorana phase would be needed to draw reasonable conclusions. Hence, measuring  $|U_{e3}|$  from neutrino-less double beta decay will be much more difficult than simply excluding part of the parameter space from a non-observation. In particular,  $|U_{e3}|^2$  should lie very close to its currently allowed  $3\sigma$ -limit.

### 3 Conclusions

Assuming that neutrinos are Majorana particles, we have performed a detailed analysis of what information on the lepton mixing matrix element  $|U_{e3}|^2$  can be gained from a (non-) observation of neutrino-less double beta decay in future experiments. After reviewing the current knowledge on the effective mass  $|m_{ee}|$ , we have shown how one can get a *lower* limit on the mixing matrix element  $|U_{e3}|^2$ , which in particular depends on the neutrino mass and the Majorana phase  $\alpha$ . However, even after including the variation by the phase as well as by the uncertainties in the oscillation parameters, there still remains a sizable excluded area in the parameter space. We have presented this for the two cases of normal and inverted mass ordering and we have also shown the impact on the sum of neutrino masses, as measured in cosmological observations. Especially for the last point, a larger area of the parameter space could be excluded in the nearer future. The precision of  $\theta_{12}$  is quite important for limits on  $|m_{ee}|$  in the regime of 0.1 eV, but much less important for smaller limits. We have also commented on the impact of errors in the Nuclear Matrix Element calculations. Depending on the specific case, this impact can be strong or weak. We have closed with showing that the “inverse”, namely a measurement of the mixing matrix element  $|U_{e3}|^2$  by an observation of neutrino-less double beta decay, is much more difficult since the errors especially due to the variation of the Majorana phase  $\alpha$  are quite large.

### Acknowledgments

This work has been supported by the DFG-Sonderforschungsbereich Transregio 27 “Neutrinos and beyond – Weakly interacting particles in Physics, Astrophysics and Cosmology” and under project number RO-2516/3-2 (W.R.), as well as by the EU program ILIAS N6 ENTApP WP1.

### References

- [1] R. N. Mohapatra *et al.*, hep-ph/0510213; R. N. Mohapatra and A. Y. Smirnov, Ann. Rev. Nucl. Part. Sci. **56**, 569 (2006) [hep-ph/0603118]; A. Strumia and F. Vissani, hep-ph/0606054.
- [2] S. Choubey, Phys. Atom. Nucl. **69**, 1930 (2006) [hep-ph/0509217].
- [3] C. H. Albright and M. C. Chen, Phys. Rev. D **74**, 113006 (2006) [hep-ph/0608137].
- [4] K. Anderson *et al.*, hep-ex/0402041.
- [5] Y. Itow *et al.*, hep-ex/0106019; D. S. Ayres *et al.* [NOvA Collaboration], hep-ex/0503053.

- [6] C. Albright *et al.* [Neutrino Factory/Muon Collider Collaboration], physics/0411123.
- [7] G. G. Raffelt, Phys. Scripta **T121**, 102 (2005) [hep-ph/0501049]; A. Dighe, Nucl. Phys. Proc. Suppl. **143**, 449 (2005) [hep-ph/0409268]; F. Cavanna, M. L. Costantini, O. Palamara and F. Vissani, Surveys High Energ. Phys. **19**, 35 (2004) [astro-ph/0311256].
- [8] Y. Farzan and A. Y. Smirnov, Phys. Rev. D **65**, 113001 (2002) [hep-ph/0201105]; P. D. Serpico and M. Kachelriess, Phys. Rev. Lett. **94**, 211102 (2005) [hep-ph/0502088]; W. Winter, Phys. Rev. D **74**, 033015 (2006) [hep-ph/0604191]; Z. Z. Xing, Phys. Rev. D **74**, 013009 (2006) [hep-ph/0605219]; W. Rodejohann, JCAP **0701**, 029 (2007) [hep-ph/0612047].
- [9] C. Aalseth *et al.*, hep-ph/0412300.
- [10] W. Rodejohann, Phys. Rev. D **62**, 013011 (2000) [hep-ph/0003149]; J. Phys. G **28**, 1477 (2002); A. Atre, V. Barger and T. Han, Phys. Rev. D **71**, 113014 (2005) [hep-ph/0502163].
- [11] H. V. Klapdor-Kleingrothaus *et al.*, Eur. Phys. J. A **12**, 147 (2001) [hep-ph/0103062].
- [12] C. Arnaboldi *et al.*, Phys. Rev. Lett. **95**, 142501 (2005) [hep-ex/0501034]; C. Bucci, talk given at LAUNCH (Low-energy, Astroparticle Underground, Neutrino physics and Cosmology in Heidelberg), Heidelberg, Germany, March 2007.
- [13] R. Arnold *et al.* [NEMO Collaboration], Phys. Rev. Lett. **95**, 182302 (2005) [hep-ex/0507083]; X. Sarazin, talk given at LAUNCH (Low-energy, Astroparticle Underground, Neutrino physics and Cosmology in Heidelberg), Heidelberg, Germany, March 2007.
- [14] M. Danilov *et al.*, Phys. Lett. B **480**, 12 (2000) [hep-ex/0002003]; K. O'Sullivan, talk given at TAUP 2007 (International Conference on Topics in Astroparticle and Underground Physics), Sendai, Japan, September 2007.
- [15] I. Abt *et al.*, hep-ex/0404039.
- [16] S. Choubey and W. Rodejohann, Phys. Rev. D **72**, 033016 (2005) [hep-ph/0506102].
- [17] Recent works are F. Feruglio, A. Strumia and F. Vissani, Nucl. Phys. B **637**, 345 (2002) [Addendum-ibid. B **659**, 359 (2003)] [hep-ph/0201291]; G. L. Fogli, E. Lisi, A. Marrone, A. Melchiorri, A. Palazzo, P. Serra and J. Silk, Phys. Rev. D **70**, 113003 (2004) [hep-ph/0408045]; hep-ph/0608060; S. Pascoli, S. T. Petcov and T. Schwetz, Nucl. Phys. B **734**, 24 (2006) [hep-ph/0505226]; A. de Gouvea and J. Jenkins, hep-ph/0507021. S. M. Bilenky, A. Faessler, T. Gutsche and F. Simkovic, Phys. Rev. D **72**, 053015 (2005) [hep-ph/0507260].
- [18] H. Minakata and H. Sugiyama, Phys. Lett. B **526**, 335 (2002) [hep-ph/0111269].

- [19] S. Pascoli, S. T. Petcov and W. Rodejohann, Phys. Lett. B **549**, 177 (2002) [hep-ph/0209059]; Phys. Lett. B **558**, 141 (2003) [hep-ph/0212113].
- [20] M. Lindner, A. Merle and W. Rodejohann, Phys. Rev. D **73**, 053005 (2006) [hep-ph/0512143].
- [21] S. Dev and S. Kumar, Mod. Phys. Lett. A **22**, 1401 (2007) [hep-ph/0607048].
- [22] A. Merle and W. Rodejohann, Phys. Rev. D **73**, 073012 (2006) [hep-ph/0603111].
- [23] S. T. Petcov, Phys. Scripta **T121**, 94 (2005) [hep-ph/0504166].
- [24] S. M. Bilenky, J. Hosek and S. T. Petcov, Phys. Lett. B **94**, 495 (1980); J. Schechter and J. W. F. Valle, Phys. Rev. D **22**, 2227 (1980); M. Doi, T. Kotani, H. Nishiura, K. Okuda and E. Takasugi, Phys. Lett. B **102**, 323 (1981); J. Bernabeu and P. Pascual, Nucl. Phys. B **228**, 21 (1983).
- [25] T. Schwetz, Phys. Scripta **T127**, 1 (2006) [hep-ph/0606060]; M. Maltoni, T. Schwetz, M. A. Tortola and J. W. F. Valle, New J. Phys. **6**, 122 (2004) [hep-ph/0405172].
- [26] S. T. Petcov, Phys. Lett. B **110**, 245 (1982).
- [27] J. A. Casas, J. R. Espinosa, A. Ibarra and I. Navarro, Nucl. Phys. B **573**, 652 (2000) [hep-ph/9910420]; K. R. S. Balaji, A. S. Dighe, R. N. Mohapatra and M. K. Parida, Phys. Rev. Lett. **84**, 5034 (2000) [hep-ph/0001310]; N. Haba, Y. Matsui and N. Okamura, Eur. Phys. J. C **17**, 513 (2000) [hep-ph/0005075]; P. H. Chankowski and S. Pokorski, Int. J. Mod. Phys. A **17**, 575 (2002) [hep-ph/0110249]; see also S. Antusch, J. Kersten, M. Lindner and M. Ratz, Nucl. Phys. B **674**, 401 (2003) [hep-ph/0305273].
- [28] For an overview see S. Hannestad, hep-ph/0602058.
- [29] M. Tegmark *et al.* [SDSS Collaboration], Phys. Rev. D **69**, 103501 (2004) [astro-ph/0310723].
- [30] A. Osipowicz *et al.* [KATRIN Collaboration], hep-ex/0109033.
- [31] R. N. Mohapatra, Phys. Rev. D **34**, 3457 (1986); K. S. Babu and R. N. Mohapatra, Phys. Rev. Lett. **75**, 2276 (1995) [hep-ph/9506354].

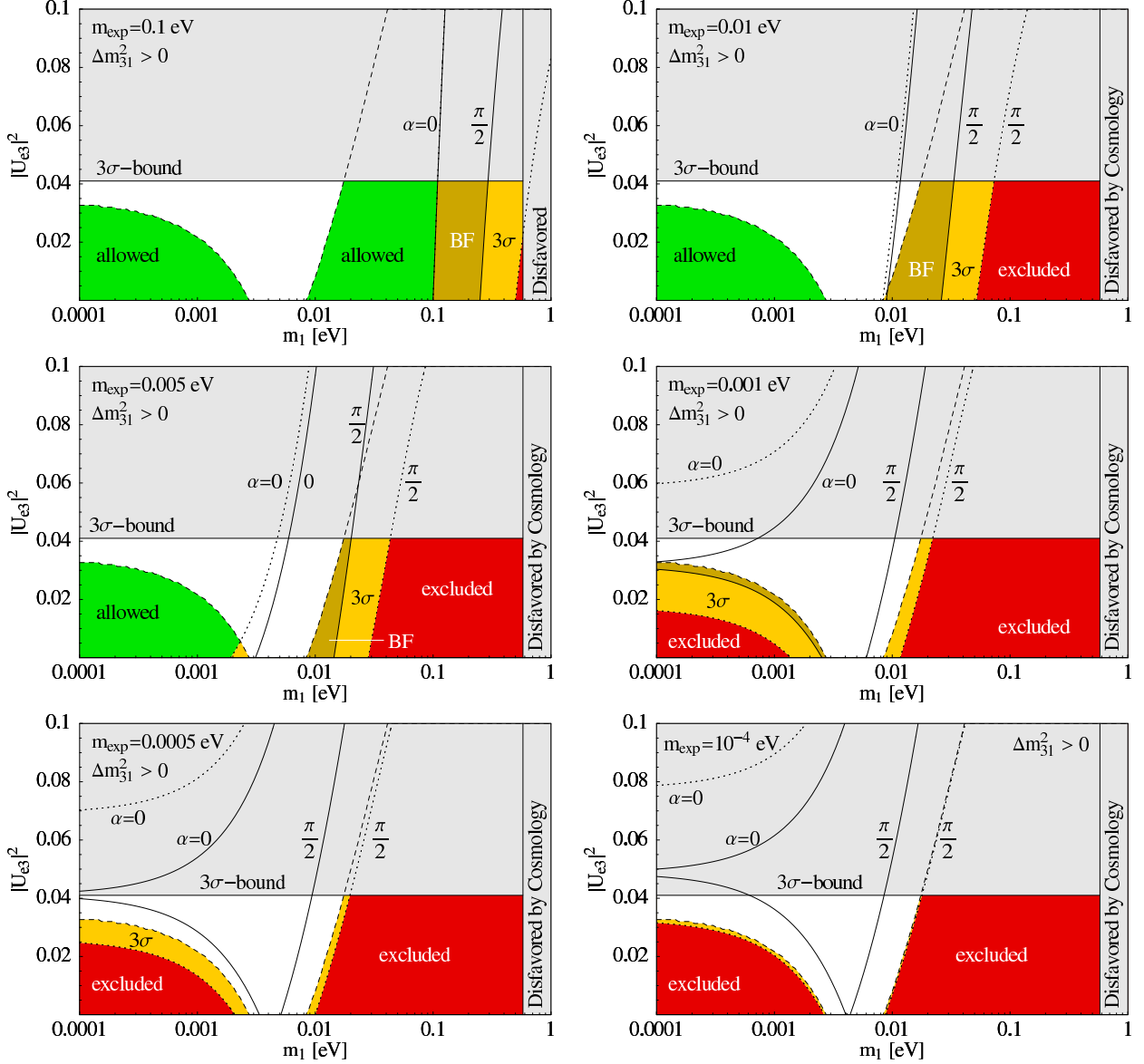


Figure 3: Normal neutrino mass ordering: Areas in the  $m_1$ - $|U_{e3}|^2$  parameter space in which information from neutrino-less double beta decay experiments could be gained. Different experimental bounds  $m_{\text{exp}}$  on the effective mass are shown, as well as the current  $3\sigma$  limit on  $|U_{e3}|^2$ . The range of the lower limit on  $|U_{e3}|^2$  is shown within solid lines in dark yellow (darkest grey) for the best-fit values (“BF”) of the oscillation parameters. The light yellow (lightest grey) area within the dotted lines is the lower limit for the  $3\sigma$ -ranges. The left and right borders of these areas correspond to  $\alpha = 0$  and  $\alpha = \pi/2$ , respectively. The red (darkest) areas are excluded, the green (medium grey) and white areas are allowed.

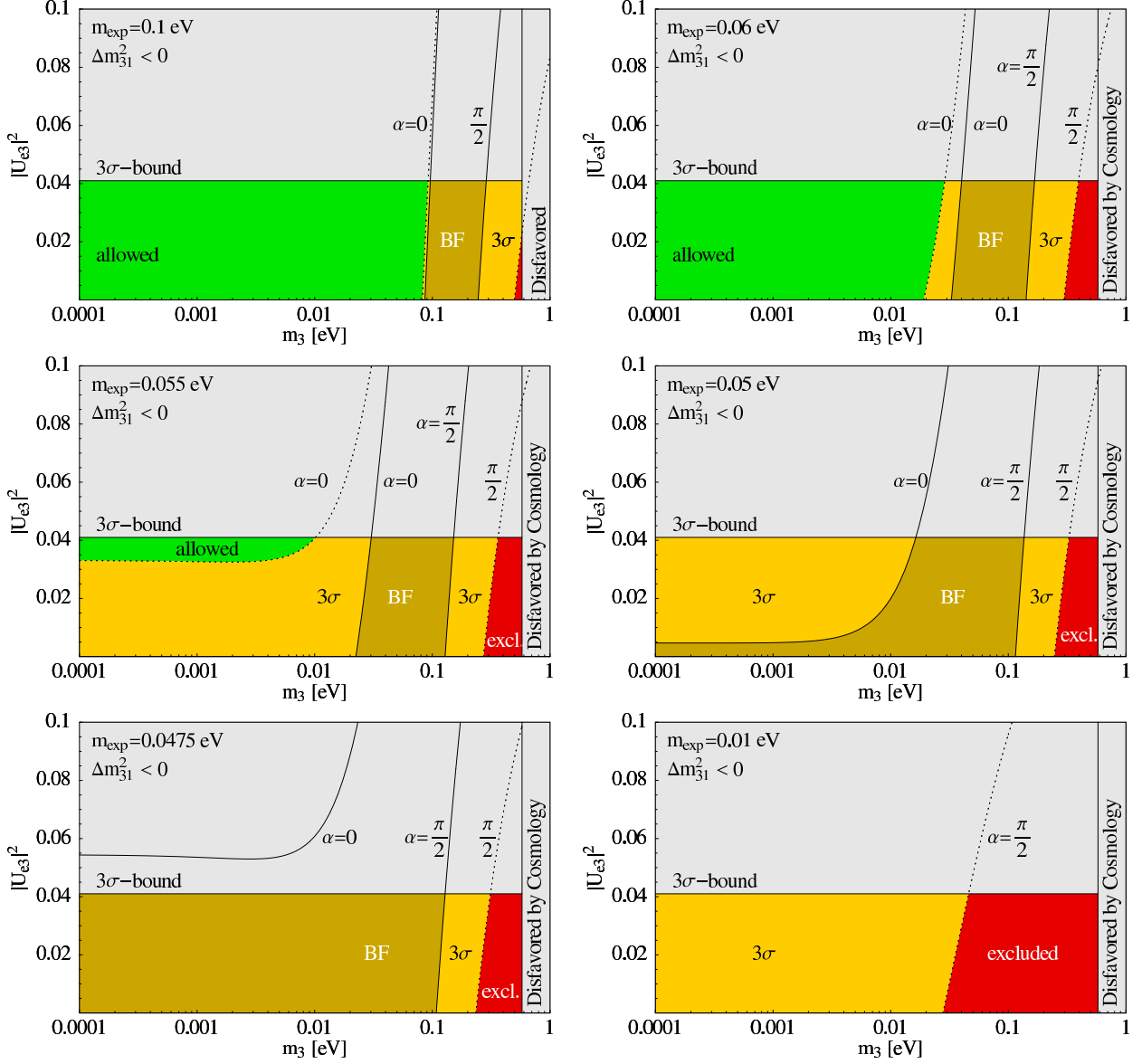


Figure 4: Inverted neutrino mass ordering: Areas in the  $m_3$ - $|U_{e3}|^2$  parameter space in which information from neutrino-less double beta decay experiments could be gained. Different experimental bounds  $m_{\text{exp}}$  on the effective mass are shown, as well as the current  $3\sigma$  limit on  $|U_{e3}|^2$ . The range of the lower limit on  $|U_{e3}|^2$  is shown within solid lines in dark yellow (darkest grey) for the best-fit values (“BF”) of the oscillation parameters. The light yellow (lightest grey) area within the dotted lines is the lower limit for the  $3\sigma$ -ranges. The left and right borders of these areas correspond to  $\alpha = 0$  and  $\alpha = \pi/2$ , respectively. The red (darkest) areas are excluded, the green (medium grey) areas are allowed.



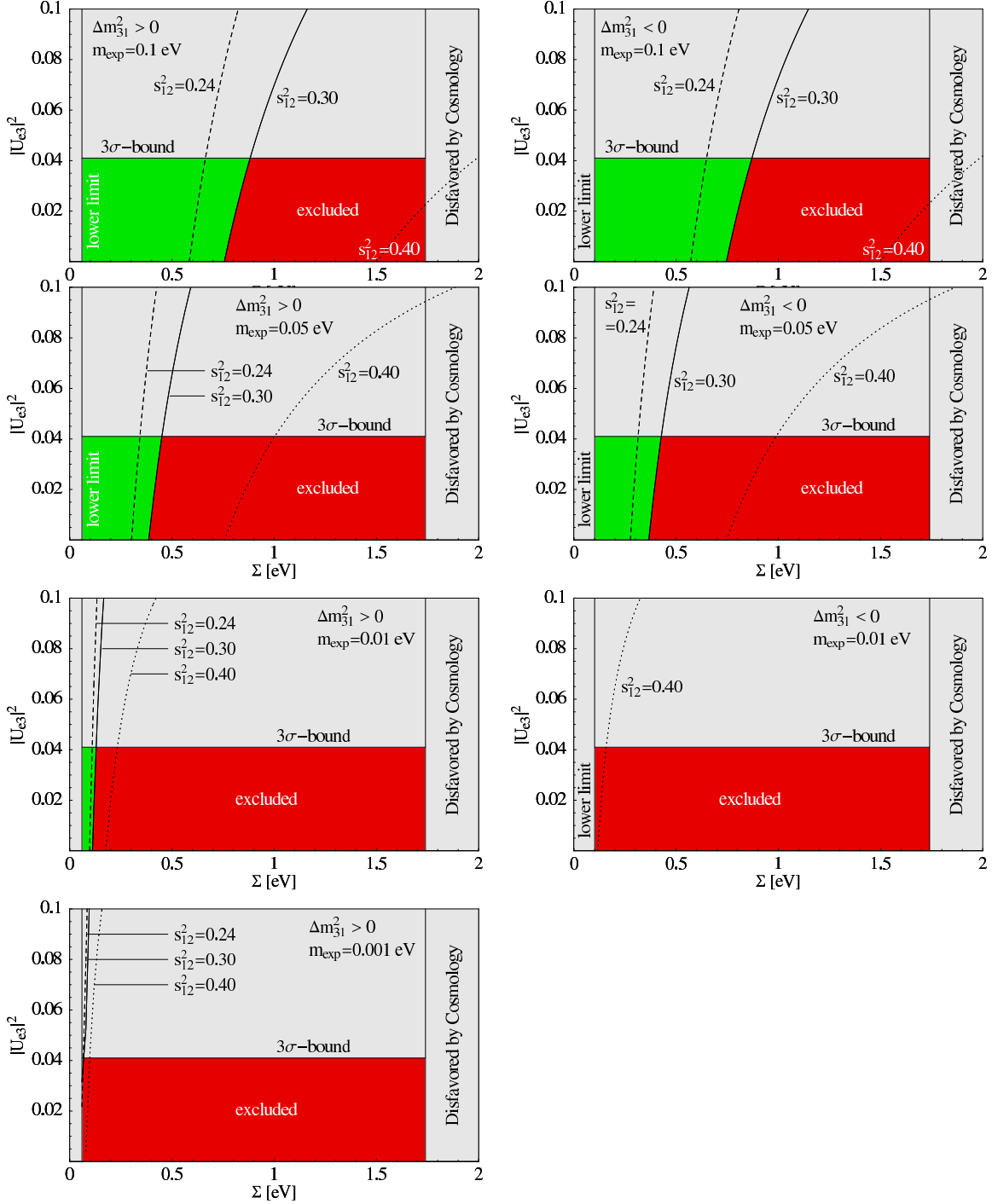


Figure 5: Excluded (red/dark grey) and allowed (green/medium grey) regions in the parameter space of  $|U_{e3}|^2$  and  $\Sigma = \sum m_i$  for a given limit  $m_{\text{exp}}$  on the effective mass and  $\sin^2 \theta_{12} = 0.30$ . The normal (inverted) mass ordering is shown in the left (right) panel. If  $\sin^2 \theta_{12} = 0.24$ , the regions would be separated by the dashed line, if  $\sin^2 \theta_{12} = 0.40$ , the regions would be separated by the dotted line. The current  $3\sigma$  limit on  $|U_{e3}|^2$ , as well as the theoretical lower and the experimental upper limit on  $\Sigma$  are also indicated.

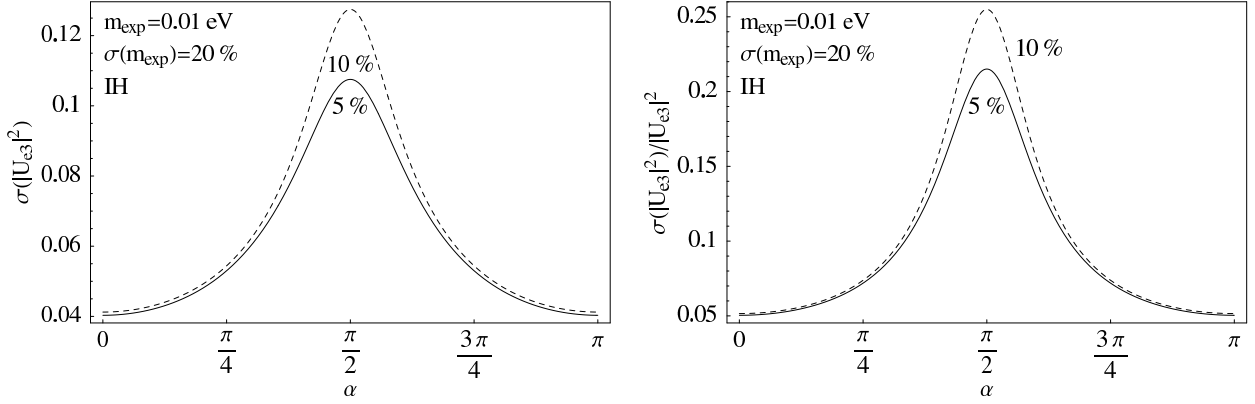


Figure 6: The absolute and relative error on  $|U_{e3}|^2$  in case of an inverted hierarchy for negligible  $m_3 |U_{e3}|^2$ .  $\Delta m_A^2$  and  $\sin^2 \theta_{12}$  are both given a relative error of 5 and 10 %, respectively. The strong dependence on  $\alpha$  is clearly visible from the plots.

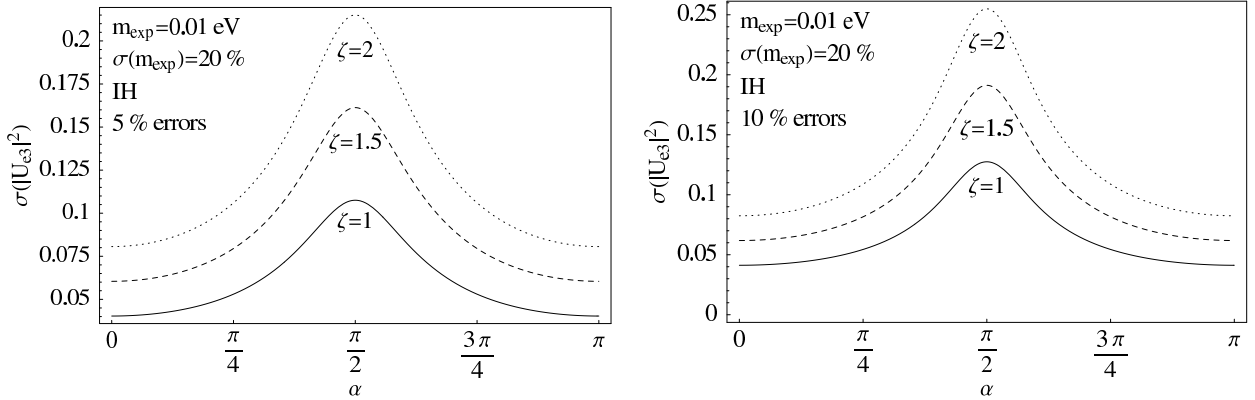


Figure 7: The influence of the nuclear matrix element uncertainty  $\zeta$  on the error of  $|U_{e3}|^2$  in case of an inverted hierarchy. The errors on  $\Delta m_A^2$  and  $\sin^2 \theta_{12}$  are again 5 and 10 %, respectively.  $\sigma(|U_{e3}|^2)$  grows linearly with  $\zeta$ .